JCTC Journal of Chemical Theory and Computation

Electron Transmission through Aromatic Molecules

Matthias Ernzerhof,* Hilke Bahmann, Francois Goyer, Min Zhuang, and Philippe Rocheleau

Département de Chimie, Université de Montréal, C.P. 6128 Succursale A, Montréal, Québec H3C 3J7, Canada

Received March 7, 2006

Abstract: A prominent feature of aromatic compounds is the ring current that can be observed indirectly in nuclear magnetic resonance experiments. This current is generated by an external magnetic field. In molecular electronics, molecules serve as conductors, and they are connected to metallic contacts that act as electron sources and electron sinks. We show that ring currents can also be found in molecular electronic devices containing cyclic π-electron systems. The circular currents are related to interference phenomena that can render the molecule impenetrable to electrons. While only small currents pass through the molecule, large internal circular currents are stimulated. We conjecture that the internal currents should result in experimentally observable magnetic moments.

1. Introduction

To consider molecules as conductors[1−4] is a subject that has recently attracted much attention. Our understanding of electron transport through molecules is presently far from complete, and the mechanisms underlying molecular conductance are only now beginning to be explored. In this context theoretical studies of molecular conductors are a valuable tool that even allow us to conceive new experiments and predict their outcome. In fact, molecular electronic devices (MEDs) have first been suggested in a theoretical article.[5] It should, however, be noted that MEDs represent an enormous theoretical challenge and that our methods of modeling MEDs[6−13] are still in their infancy. In particular correlation effects are difficult to account for properly.[14]

An interesting question that arises in molecular electronics is whether established concepts of chemistry are still useful in the analysis of MEDs. Here, we consider the notion of the ring current that is a prominent feature of aromatic systems. Employing the simple Hückel model, we investigate the conductance of benzene and coronene, and we find indeed that ring currents are crucial to rationalize the transmission of electrons through aromatic molecules. We demonstrate that benzene and coronene exhibit prominent negative interference effects that are related to ring currents. Investigations similar to ours have already been performed for related systems.[15] In ref 16 the electron transmission probability for the benzene molecule with wires attached to it is discussed. An analysis of the molecular orbitals is presented to explain the interference phenomena observed. Maybe the most important advance made here, in comparison to earlier work, is that we analyze the internal current distribution in the molecule. We believe that this distribution is essential to fully understand the current transport through MEDs. From the molecular current distribution, we are able to calculate the magnetic moment generated by the ring currents. We predict that coronene, with a voltage applied to it, could generate a magnetic moment of several μ_B, where $\mu_B = (e\hbar/2m_e)$ is Bohr's magneton. The determining feature of the molecular conductors examined here is their circular delocalized π-electron system. This type of system continues to attract attention. Recently, the behavior of circular molecular conductors in magnetic fields has been studied (for review see ref 17). Three-terminal circular logic gates have been proposed,[18] and the dependence of the transmittance on the arrangement of the leads attached to a circular conductor has been investigated.[19]

In the remainder of this paper we use atomic units ($m_e = e^2 = \hbar = 1$), unless indicated otherwise.

2. Summary of Theoretical Concepts

A basic tool of molecular electronics is Landauer's formula[20] for the ballistic conductance $g(E)$

10.1021/ct600087c CCC: $33.50
Published on Web 07/04/2006

$$g(E) = \frac{1}{2\pi} T(E) \tag{1}$$

(Note that the conductance quantum (e^2/h) reduces to ($1/2\pi$) in atomic units.) If electron−electron interaction is considered through an effective single-particle approach, the transmission probability $T(E)$ can be obtained according to[6−8]

$$T(E) = Tr(\mathbf{\Gamma}_R \mathbf{G}^r \mathbf{\Gamma}_L \mathbf{G}^a) \tag{2}$$

where $\mathbf{G}^{a(r)}(E)$ is the advanced (retarded) Green's function of the entire system. $\mathbf{\Gamma}_{L(R)}(E) = 2\pi \mathbf{M}_{L(R)} \delta(\mathbf{H}_{L(R)} - E) \mathbf{M}^{\dagger}_{L(R)}$ contains the density of state operator $\delta(\mathbf{H}_{L(R)} - E)$ of the left (right) contact multiplied by the operator $\mathbf{M}_{L(R)}$ that couples the left (right) contact to the molecule. Numerous strategies are available to implement (see e.g., refs 10−12 and 21−23) this formula. Here we are interested in the properties of delocalized π systems, and it is known that the qualitative features of such systems can be reproduced with a simple Hückel model. Furthermore, we assume that the voltage applied to the system is small, such that its polarizing effect on the orbitals and thus on $T(E)$ can be neglected. Finally, we suppose that the contacts are identical, that they have a constant density of states (this is sometimes called the wide band limit), and that they couple to the molecule only through the molecular atom that is attached to the chain. In this case, $\mathbf{\Gamma}_{L(R)}(E)$ reduces[24] to a matrix with a single element. This element is treated as a parameter in our work, and we set it equal to the hopping matrix element used in the molecule. By varying the coupling strength, we ensured that the qualitative conclusions drawn here are not sensitive to the exact value of this parameter. We stress that in the present work we do not attempt to describe quantitative but rather qualitative effects that are robust with respect to the choice of the model parameters and with respect to the choice of the theoretical method employed to calculate $T(E)$. The simple approach just described makes it possible to quickly examine $T(E)$ of numerous structures. All the T versus E curves presented here have been generated with this scheme, the exception being Figure 9 described in the Appendix.

One of the main aims of our work is to use the internal current distribution as a tool to understand molecular conductance. All the current distributions presented in the following have been obtained with a method that we developed recently and that will be described in detail in a forthcoming publication.[25] Here we provide a short outline. We consider a finite model of a MED, the Hamiltonian of which contains a complex one-particle potential $\hat{\Sigma}$

$$\hat{H} = \hat{T} + \hat{v} + \hat{\Sigma} \tag{3}$$

The Hamiltonian operator in eq 3 is non-Hermitian, nevertheless it permits the development of a consistent quantum mechanics.[25] To show that the Hamiltonian in eq 3 enables us to describe an MED with a stationary current passing through, we consider a one-dimensional contact along the x axis that extends from $-\infty$ to 0. This contact represents the left contact of a MED, and, at $x = 0$, we attach the molecule to it. In the left contact, sufficiently far away from the molecule, the wave function φ is a combination of a forward going Bloch wave $\varphi^+(x)$ and a backward going Bloch wave $\varphi^-(x)$

$$\varphi(x) \overset{\text{left contact}}{=} a\varphi^+(x) + b\varphi^-(x) \tag{4}$$

Since we want our model system to be finite, we multiply $\varphi(x)$ by a damping factor $f^{L}(x)$. This function takes a value of one in the region that includes the molecule and beyond ($x \rightarrow \infty$), and it drops to zero inside of the left contact. We define

$$\phi(x) \overset{\text{left contact}}{=} f^{L}(x)\, \varphi(x) \tag{5}$$

The damping factor $f^{L}(x)$ is of course not unique, but this does not pose a problem for our approach. Inserting ϕ into the stationary Schrödinger equation

$$\left(-\frac{1}{2}\Delta + \hat{v} + \hat{\Sigma}\right)\phi \overset{\text{left contact}}{=} E\phi \tag{6}$$

and subsequent inversion of this equation yields an expression for the potential $\hat{\Sigma} = \hat{\Sigma}_L + \hat{\Sigma}_R$ in the left contact

$$\Sigma_L(x) \overset{\text{left contact}}{=} \frac{\Delta\phi(x)}{2\phi(x)} - v(x) + E \tag{7}$$

Multiplication of ϕ by a constant does not change the value of the potential $\hat{\Sigma}_L$. This allows us to eliminate the coefficient a in eq 4, and we are left with one unknown complex parameter $r = b/a$ in $\hat{\Sigma}_L$. Note that for $|r| = 1$ there is no net current flow since forward and backward going Bloch wave have the same weight. In this case $\hat{\Sigma}_L$ is a real potential. If the molecule is transparent ($T = 1$), then $r = 0$. For $|r| \neq 1$, $\hat{\Sigma}_L$ is complex.

In the right contact that starts at $x = l$, we only have a forward going Bloch wave (φ^+) that we damp by a function $f^{R}(x)$ that drops to zero at some distance from the molecule. Similar to $f^{L}(x)$, $f^{R}(x)$ is equal to one in the physical region including the molecule and beyond ($x \rightarrow -\infty$). We have

$$\phi(x) \overset{\text{right contact}}{=} c f^{R}(x) \varphi^+(x) \tag{8}$$

Inversion of the Schrödinger equation with the wave function in eq 8 yields $\hat{\Sigma}_R$. The parameter c cancels out of the equation for $\hat{\Sigma}_R$.

Equation 7 allows us to calculate $\hat{\Sigma}_L$ as a function of the parameter r that in turn depends on the energy E. r is directly related to $T(E)$ by

$$T(E) = 1 - |r(E)|^2 \tag{9}$$

The remaining question is then how to obtain r? The condition that an eigenvalue of the model Hamiltonian in eq 3 is identical to the energy chosen in the potential $\hat{\Sigma}_{L(R)}$ suffices[13,25] to determine r. Note that the energy (and the eigenvalue of $\hat{H}$) of interest is real. The ideas just described are readily applied to the Hückel model.[25] The contacts, represented by infinite chains of equidistant atoms, are replaced by complex potentials. From the wave function that we obtain, we calculate the current distribution (using eq 10, given below). We verified that our model Hamiltonian

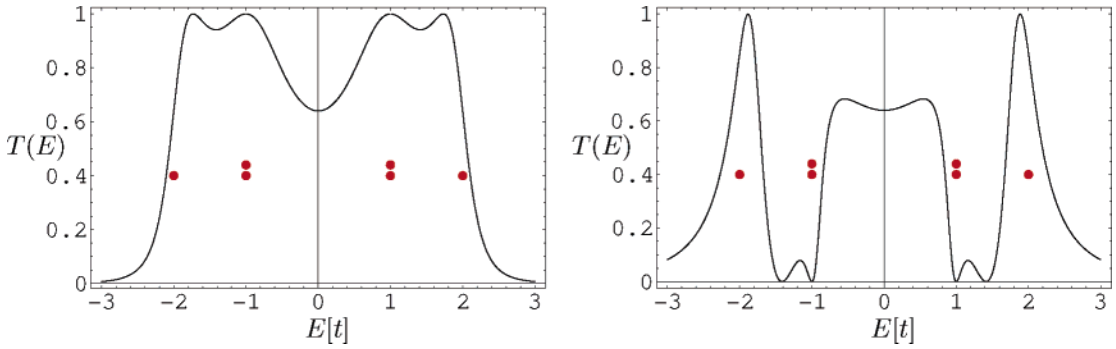

Figure 1. The transmission probability $T(E)$ of the benzene molecule with the leads attached in the para position (left) and in the ortho position (right). The dots indicate the positions of the orbital energies in the unperturbed molecule. The energy is given in units of the hopping parameter t.

yields the exact $T(E)$ of the underlying infinite system in which the contacts have not been replaced by $\hat{\Sigma}$.

As mentioned above, the $T(E)$ curves presented are obtained from eq 2 in the wide band limit. The features discussed here do not depend on which method we use, however. To demonstrate this, in the Appendix, $T(E)$ obtained from our non-Hermitian model Hamiltonian is compared to $T(E)$ obtained from eq 2.

In the Hückel model, that we employ in the present work, there are no continuous spatial variables. Instead, all equations are formulated in a finite-dimensional vector space. While the formulas given above can be transferred in a straightforward fashion to the Hückel model, it is useful to provide the expression for the current density. We find that the current density along a bond joining atoms k and l is

$$j_{k\to l} = i(c_k^* t c_l - c_l^* t c_k) \tag{10}$$

where the hopping matrix element between the atoms is t, and c_k is an orbital coefficient. Between two bound atoms, the Hückel model is effectively a one-dimensional model, and, in one dimension, the current density and the current are identical. The divergence of the current ($\nabla\mathbf{j}$) in the Hückel model is simply the difference between the current flowing in to and out of an atom. Apparently, $\nabla\mathbf{j}$ should be zero unless the atom in question has an imaginary matrix element. Finally, we list the Hückel parameters employed in the calculations. The on-site energies are set to zero. The hopping parameter in the contact chains is $1.4t$, where t is the hopping parameter in the molecule. The coupling matrix element between the contact and the molecule is also t.

3. Benzene Molecule

Using the tools discussed above, we now turn to the discussion of transmission probability through the prototypical aromatic molecule, namely benzene. It is well-known that the HOMO and LUMO of this molecule are doubly degenerate. The degeneracy originates from the fact that electrons with the same absolute value of momentum circulate left or right around the ring. If leads are added in the para position, the degeneracy is lifted, and we obtain two orbitals that are oriented such that one of them connects the two leads on opposite sides of the molecule and the second one is zero on the atoms connected to the leads. This behavior is isomorphic to the problem of two p orbitals: one

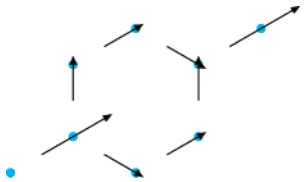

Figure 2. Current distribution in para-connected benzene at $E = -1.03$. At this energy, the molecule transmits well. This current distribution persists over the entire energy range except at $E = \pm 1$, where the current distribution is zero. Note that this feature at $E = \pm 1$ is not reproduced by the Green's function calculation of $T(E)$.

with magnetic quantum number $m_z = 1 (p_1)$ and one with magnetic quantum number $m_z = -1 (p_{-1})$. An appropriate perturbation splits the degeneracy and yields a p_x- and a p_y-type orbital. The p_y-type orbital being zero along the direction of the p_x orbital. The transmission probability of the para-benzene is displayed in Figure 1. The curve can easily be understood in terms of the analysis presented above. Due to the symmetry of the perturbation, one of the molecular HOMOs is essentially excluded from the conductance path, and the other one yields a peak reaching up to one. We employ our method described above to generate a current flow through the molecule. A typical picture of the internal current distribution is shown in Figure 2. The arrows, indicating direction and magnitude of the current, have been normalized such that the longest arrow in each figure has a certain fixed length. Although this current distribution has been obtained for a particular energy ($E = -1.03$), it is representative for the entire energy range. After entering the molecule, the current splits symmetrically to pass through the π system. For the para-benzene, our findings agree essentially with ref 16, with the exception that we do not obtain the drop to zero in $T(E)$ at the position of the molecular HOMO and LUMO. These gaps in $T(E)$ are of zero width,[16] and they are probably eliminated by the level broadening inherent in the Green's function formalism (eq 2) used here to obtain $T(E)$. Features of zero width in $T(E)$ have probably no observable consequences.

With the leads placed in the ortho or the meta position, the degeneracy of the molecular HOMO is also lifted, but there is no effective elimination of either resulting orbital from the conductance path. $T(E)$ touches zero when E passes through the molecular HOMO energy. This is an indication

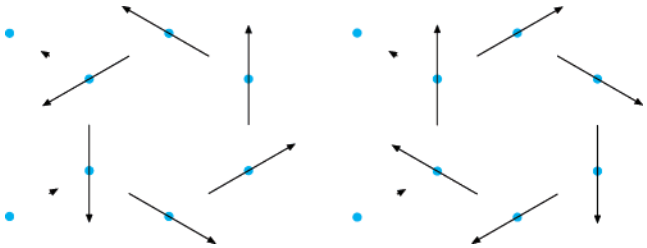

Figure 3. Current distribution in ortho-connected benzene. The two pictures show the current distribution slightly below (left) and above (right) $E = -1$. Note that the incoming and outgoing current is almost zero and that the direction of the current flow changes from one figure to the other.

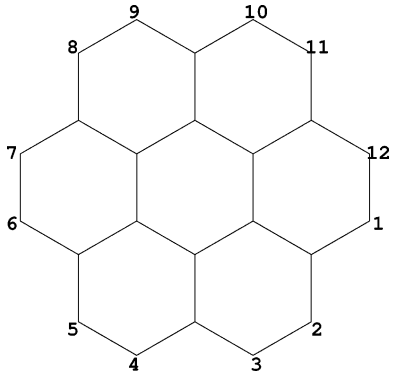

Figure 4. The carbon backbone of coronene. For the purpose of this article, the 1−3 position will be referred to as ortho, and the 1−7 position will be referred to as para.

of a strong negative interference effect that calls for a detailed investigation. The intramolecular current distribution slightly below and above $E = -1$ is shown in Figure 3. Below $E = -1$ there is a large counterclockwise circular current in the benzene molecule. This circular current yields only a small net transport through the molecule. Slightly above $E = -1$, we observe a similar phenomenon, but interestingly, the circular current is turning in the opposite direction. As a consequence of these opposing currents, there is a certain intermediate energy at which the circular currents cancel exactly such that no current flow through or inside of the molecule is obtained. At energies around that of the degenerate HOMOs, these orbitals essentially determine the internal current distribution. One of the HOMOs describes an electron moving clockwise, and the other one describes an electron moving counterclockwise. In the MED the degeneracy of the HOMOs is split, leading to the counter rotating electrons at different energies. We were not able to identify a simple criterion that would determine the orientation of the current circulation without having to perform the full calculation of the current distribution.

For energies close to ± 1.4 there are additional zeros in $T(E)$. An inspection of the current distribution reveals that there is again a change in direction of a circular current, very similar to what is displayed in Figure 3. However, this interference is not associated with a resonance of a degenerate orbital, rather it is an interference between the tails of two resonances at different energies. We varied the parameters in our Hückel description, in particular the coupling between the contact and the molecule, to confirm that there are indeed additional interferences due to overlapping tails of resonances.

In the meta-benzene, that we do not discuss here, we also find strong interference effects similar to ortho-benzene, yet no new features are observed.

For the ortho-benzene, our results are also in agreement with the analysis of ref 16. These authors explain the interferences in terms of the phase and amplitude of the scattering wave function. This is a more general approach that does not bring to light the peculiar nature of the interference in the benzene, however.

4. Coronene Molecule

In Figure 4 we show the carbon backbone of the coronene molecule. For the purpose of this article, we define the 1−7 position to be para. Similar to benzene, coronene has a doubly degenerate HOMO and LUMO.

Connecting the leads in the para position leads to transmission features (Figure 5) analogous to the ones observed for the para-benzene. The degenerate molecular HOMO is split by the interaction with the contacts, and one of the resulting orbitals is eliminated from the conductance path, i.e., its orbital coefficients are zero in the 1- and 7-positions. The remaining orbital gives rise to a conductance channel that is completely open ($T(E) = 1$). The other doubly degenerate orbitals generate analogous transmission features. Interestingly, we also find transmission probabilities of zero for the para arrangement. To investigate this phenomenon, we study the current distribution at $E \approx -1.6$ (Figure 6).

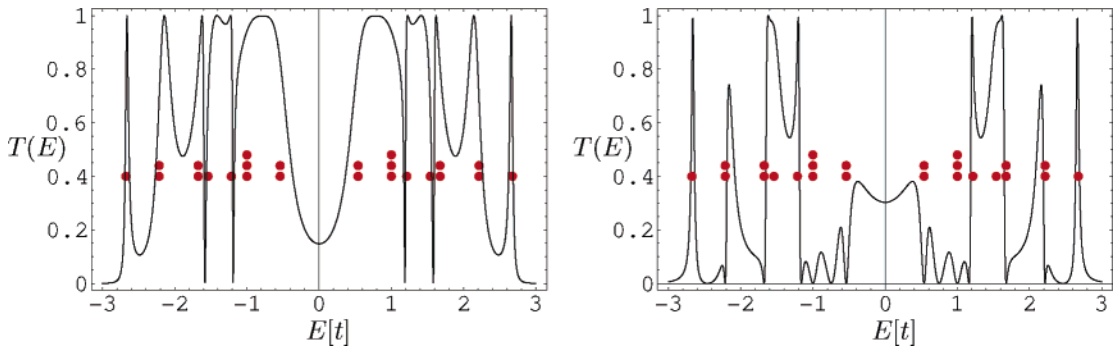

Figure 5. The transmission probability $T(E)$ of the coronene molecule with the leads attached in the para position (left) and in the ortho position (right). The dots indicate the positions of the orbital energies in the unperturbed molecule.

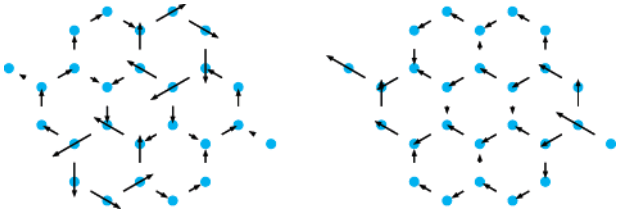

Figure 6. Intramolecular current distribution in the para-coronene for $E \approx -1.6$ (left) and $E \approx -0.9$ (right).

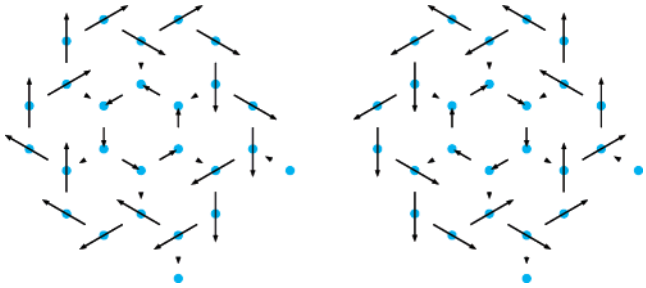

Figure 7. Shown are the current distributions slightly below (left) and above (right) $E \approx -0.6$. Note that the direction of the circular current changes from one figure to the other.

In the left panel of Figure 6, we see that there are two benzene-type substructures (upper right and lower left) that carry circular currents. The zero in $T(E)$ is due to the fact that at this particular energy the current is localized in a fragment of the molecule that does not include the atoms attached to the leads. The same explanation applies to the narrow feature at $E \approx \pm 1.2$.

To complete the discussion of the para-coronene, in Figure 6 we also show the current distribution at $E = \pm 0.9$. $T(E)$ is close to one for this energy. The entire molecule makes a coherent contribution to the electron transport. There is a slight preference for the current to pass through the antracene-type substructure joining the entry and exit point.

Similar to what we observed for the benzene molecule, there is a strong interference signature in $T(E)$ (Figure 5) of ortho coronene for energies around the molecular HOMO. There are again two pathways for electron transmission associated with orbitals slightly below and above the HOMO energy of the isolated molecule. As in the benzene, there is an intermediate energy at which the two pathways superimpose such as to annihilate each other. As a consequence, we observe complete destructive interference. To illustrate this point, in Figure 7 we show the current distribution at an energy slightly below and above the energy of the HOMO of the isolated molecule. There is a strong clockwise current flow in the outer ring and a counterclockwise current flow in the inner ring that is reversed upon passage through the HOMO energy. In the ortho-coronene there are not only resonant but also off-resonant destructive interferences. At $E \approx \pm 1.2$ we find such a feature that is associated with a change in direction of a circular current. For $E = \pm 1$ we find three degenerate orbitals in the molecule. At this energy, we observe another zero in $T(E)$. Inspection of $\mathbf{j}$ reveals that there is an isolated circular current localized in the center benzene ring that changes direction upon passage through $E = \pm 1$.

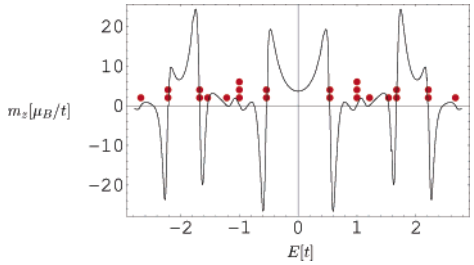

Figure 8. Magnetic moment generated by the internal current distribution of energy E. Three prominent oscillations are visible in each half of the figure. They are generated by circulating electrons changing direction. The corresponding states originate from doubly degenerate molecular orbitals, the position of which is indicated by red dots.

While we used the same Hückel parameters in the calculations for coronene and benzene, the peaks for the coronene are much narrower than the peaks for benzene. This is because the coronene is larger than the benzene, and the coronene orbitals are thus less perturbed by the addition of the contacts.

We considered all the other possible sites for wire attachments in the coronene molecule. In all cases we find similar interference patterns as the ones described here.

5. Observable Consequences of the Predicted Circular Currents

In the previous sections we showed that the concept of a ring current plays an important role in the interpretation of the transmission probabilities. We saw that large circular currents may be induced by the external contacts even if little current is flowing through the molecule. These circular currents should generate a magnetic moment $\mathbf{m}$, normal to the molecular plane, that might be observable. To further elaborate on this issue, we calculate $\mathbf{m}$ as a function of the energy for the coronene. We are only interested in the contribution from the molecule, and we neglect contributions to $\mathbf{m}$ due to the contacts. The magnetic moment of a wire in a plane with current I passing through is[26]

$$\mathbf{m} = \frac{1}{2}\int \boldsymbol{r} \times d\mathbf{I} \tag{11}$$

where $d\mathbf{I}$ is a vector that points in the direction of the wire. The length of $d\mathbf{I}$ is scaled by I. Evaluation of this formula within the Hückel model yields[27]

$$\mathbf{m}(E) = \frac{1}{2}\sum_{i>k} j_{ik}(E)(\boldsymbol{r}_i \times \boldsymbol{r}_k) \tag{12}$$

$j_{ik}(E)$ is the current flowing along the bond (ik) in an orbital with energy E. $\boldsymbol{r}_i$ and $\boldsymbol{r}_j$ are the positions of atom i and j, respectively. Since coronene is planar, $\mathbf{m}(E)$ is perpendicular to the molecular plane, parallel to the z-axis. A plot of $m_z(E)$ is shown in Figure 8. In agreement with the observation of circular currents of rapidly changing orientation, there are strong variations in $m_z(E)$. For negative energies, we observe three large oscillations. These oscillations are generated by electrons circulating in the molecule in opposing directions, depending on their energy. Note that the large circular

currents, i.e., large magnetic moments are associated with doubly degenerate molecular orbitals. As mentioned earlier, the 3-fold degenerate molecular level yields a circular current in a benzene-type substructure. Correspondingly, we observe a small oscillation in m_z at $E = \pm 1$. We should point out that the calculation of m_z is only approximately correct. Strictly speaking, the magnetic moment is only well defined for a closed charge distribution.[26] In our case, the external leads (that we neglected) also give rise to a contribution to the magnetic moment. Close to the points of destructive interference however, the current in the leads approaches zero, and thus the formula for the magnetic moment becomes correct.

If we assume that the voltage V applied to the molecule is small, such that $m_z(E)$ does not change as a function of V, then the total magnetic moment can be obtained from

$$m_z(V) = \int_{-E_1}^{E_1} dE m_z(E) \tag{13}$$

where $\Delta E = 2E_1 = eV$, and e is the electron charge.

In principle it is possible to assign values to the parameters in our Hückel treatment and to calculate $m_z(V)$. Instead, we give a simple estimate. We suppose that the integral in eq 13 extends from the HOMO to the LUMO. The magnetic moment of a circular current is given by

$$\mu = IA \tag{14}$$

where I is the current, and A is the surface area encircled by the current. The current can be obtained by

$$I = \frac{eh}{2\pi mr\lambda} \tag{15}$$

where e is the electron charge, m is the electron mass, r is the radius of the circle described by the current I, and λ is the electron wavelength. λ can be determined by inspection of the coronene π-electron system. The HOMO of coronene has an alternating bonding and antibonding structure. With this in mind, the electron wavelength in the HOMO is estimated to be four bond lengths (5.6 Å). By using eqs 14 and 15, we obtain a magnetic moment of about 4.1 μ_B for an electron circling on the outer ring of coronene. Because of spin degeneracy, this value has to be multiplied by a factor of 2. Furthermore, to estimate $m_z(V)$ in eq 13, where the moment is generated by the HOMO and the LUMO, we multiply by an additional factor of 2. Altogether, we obtain $m_z \approx 16.4\mu_B$. This is a magnetic moment that might be observable experimentally.

6. Discussion and Conclusion

For the representative aromatic molecules considered, we find that the most striking features in $T(E)$ are caused by negative interferences. By analyzing the internal current distribution, we demonstrate that often the interferences are related to opposing ring currents. Other interferences lead to localization of the current distribution in a substructure of the molecule that excludes atoms connected to the contacts.

One of the few studies of intramolecular current distributions has been performed for the C60 molecule.[27] Circular currents have also been observed in this system. In ref 27 and in our own studies on C60, it was found that for energies around the HOMO/LUMO there are no "global" current circulations, rather vortices are observed in five-membered rings. We conclude that the magnetic moments generated in C60 are much weaker than the ones reported here. (The moment is proportional to the area enclosed by the current.)

There is presently a renewed interest[28] in large circular π-electron systems because of their potential to exhibit the Aharonov-Bohm effect.[29] The giant circular molecule with $\approx$12 nm in diameter recently synthesized,[28] and systems such as Kekulene[30] might produce enormous magnetic moments in molecular conductance experiments. Although only small currents will pass through the molecule at the appropriate insertion energy, we predict that there will be large intramolecular currents. Until now, it appears that only para connected aromatic molecules have been investigated experimentally. The large molecules mentioned might permit a nonpara connection to the contacts that is difficult to realize with benzene and other small systems.

In the present work, we neglected the polarizing effect that an applied external field would have on the electronic structure. A finite applied voltage might considerably distort the molecular orbitals and hinder the appearance of circular currents. Furthermore, variations in the number of π-electrons (due to the contacts) can introduce geometry changes that also reduce the π-electron delocalization. However, recent progress[31] in achieving large gate fields might help in the experimental verification of the predicted circular currents. This is because gating allows a line up of the molecular orbitals with the Fermi level of the contacts. Thus it should not be necessary to apply a large voltage to the system in order to generate the predicted ring currents.

Acknowledgment. We would like to acknowledge the financial support provided by NSERC through Grant 238404-03.

Appendix: Comparison of Transmission Probabilities Obtained with Different Methods

To generate the $T(E)$ curves, we employed the Green's function method eq 2, describing the contacts by a single model parameter. To show that this approximation does not affect the qualitative features discussed here, we compare $T(E)$ (Figure 9) of a system with infinite chains of atoms as contacts (used to generate the internal current distribution) to the more approximate results.

If infinite one-dimensional contacts are used, then we have a band of states with a width of $2.8t$. The density of states of these chains is flat around the Fermi energy ($E = 0$), increases sharply towards the band edges to drop to zero precipitously beyond $E = \pm 2.8t$. This explains why the two curves deviate more in the outer left and right part of the figure. The approximate treatment of the contact used to generate the solid curve corresponds to a constant density of states. The zeros in $T(E)$ and its qualitative features are shared by both approaches.

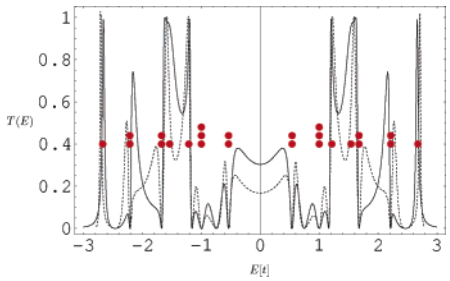

Figure 9. Comparison of transmission probabilities obtained from the Green's function approach (eq 2) with simplified contacts (solid curve) and from the non-Hermitian model Hamiltonian in eq 3 (dashed curve). The latter method yields results identical to those of the Green's function method with infinite one-dimensional contacts.

References

(1) Joachim, C.; Gimzewski, J. K.; Aviram, A. *Nature* **2000**, *408*, 541−548.

(2) Nitzan, A. *Annu. Rev. Phys. Chem.* **2001**, *52*, 681−750.

(3) Nitzan, A.; Ratner, M. A. *Science* **2003**, *300*, 1384−1389.

(4) Heath, J. R.; Ratner, M. A. *Phys. Today* **2003**, *56*, 43−49.

(5) Aviram, A.; Ratner, M. A. *Chem. Phys. Lett.* **1974**, *29*, 277−283.

(6) Meir, Y.; Wingreen, N. S. *Phys. Rev. Lett.* **1992**, *68*, 2512−2515.

(7) Mujica, V.; Kemp, M.; Ratner, M. A. *J. Chem. Phys.* **1994**, *101*, 6849−6855.

(8) Datta, S. *Electronic Transport in Mesoscopic Systems;* Cambridge University Press: 1995.

(9) Lang, N. D. *Phys. Rev. B* **1995**, *52*, 5335−5342.

(10) Xue, Y.; Datta, S.; Ratner, M. A. *J. Chem. Phys.* **2001**, *115*, 4292−4299.

(11) Taylor, J.; Guo, H.; Wang, J. *Phys. Rev. B* **2001**, *63*, 121104-(R)/1−4.

(12) Brandbyge, M.; Mozos, J.-L.; Ordejón, P.; Taylor, J.; Stokbro, K. *Phys. Rev. B* **2002**, *65*, 165401/1−17.

(13) Ernzerhof, M.; Zhuang, M. *J. Chem. Phys.* **2003**, *119*, 4134−4140.

(14) Zhuang, M.; Rocheleau, P.; Ernzerhof, M. *J. Chem. Phys.* **2005**, *122*, 154705/1−6.

(15) Walter, D.; Neuhauser, D.; Baer, R. *Chem. Phys.* **2004**, *299*, 139−145.

(16) Sautet, P.; Joachim, C. *Chem. Phys. Lett.* **1988**, *153*, 511−516.

(17) Hod, O.; Rabani, E.; Baer, R. *Acc. Chem. Res.* **2006**, *39*, 109−117.

(18) Yi, J.; Cuniberti, G. *Ann. N. Y. Acad. Sci.* **2003**, *1006*, 306−311.

(19) Yi, J.; Cuniberti, G.; Porto, M. *Eur. Phys. J. B* **2003**, *33*, 221−225.

(20) Landauer, R. *Philos. Mag.* **1970**, *21*, 863−867.

(21) Cuevas, J. C.; Levy Yeyati, A.; Martín-Rodero, A. *Phys. Rev. Lett.* **1998**, *80*, 1066−1069.

(22) Brandbyge, M.; Kobayashi, N.; Tsukada, M. *Phys. Rev. B* **1999**, *60*, 17064−17070.

(23) Ke, S. H.; Barranger, H. U.; Yang, W. *Phys. Rev. B* **2003**, *70*, 085410/1−12.

(24) Hall, L. E.; Reimers, J. R.; Hush, N. S.; Silverbrook, K. *J. Chem. Phys.* **2000**, *112*, 1510−1521.

(25) Goyer, F.; Ernzerhof, M. Manuscript in preparation.

(26) Jackson, J. D. *Classical Electrodynamics;* John Wiley & Sons: Ltd.: 1998.

(27) Nakanishi, S.; Tsukada, M. *Phys. Rev. Lett.* **2001**, *87*, 126801/1−4.

(28) Mayor, M.; Didschies, C. *Angew. Chem., Int. Ed.* **2003**, *42*, 3176−3179.

(29) Aharonov, Y.; Bohm, D. *Phys. Rev.* **1959**, *115*, 485−491.

(30) Diederich, F.; Staab, H. A. *Angew. Chem., Int. Ed.* **1978**, *17*, 372−374.

(31) Xu, B.; Xiao, X.; Yang, X.; Zang, L.; Tao, N. *J. Am. Chem. Soc.* **2004**, *127*, 2386-2387.

CT600087C